PALEOANTHROPOLOGY

A Middle Pleistocene *Homo* from Nesher Ramla, Israel

Israel Hershkovitz[1,2]*†, Hila May[1,2]*†, Rachel Sarig[2,3]*†, Ariel Pokhojaev[1,2,3], Dominique Grimaud-Hervé[4], Emiliano Bruner[5], Cinzia Fornai[6,7], Rolf Quam[8,9,10], Juan Luis Arsuaga[9,11], Viktoria A. Krenn[6,7], Maria Martinón-Torres[5,12], José María Bermúdez de Castro[5,12], Laura Martín-Francés[5,12], Viviane Slon[1,2,13], Lou Albessard-Ball[4,14], Amélie Vialet[4], Tim Schüler[15], Giorgio Manzi[16], Antonio Profico[14,16], Fabio Di Vincenzo[16]‡, Gerhard W. Weber[7,17]†, Yossi Zaidner[18,19]†

It has long been believed that Neanderthals originated and flourished on the European continent. However, recent morphological and genetic studies have suggested that they may have received a genetic contribution from a yet unknown non-European group. Here we report on the recent discovery of archaic *Homo* fossils from the site of Nesher Ramla, Israel, which we dated to 140,000 to 120,000 years ago. Comprehensive qualitative and quantitative analyses of the parietal bones, mandible, and lower second molar revealed that this *Homo* group presents a distinctive combination of Neanderthal and archaic features. We suggest that these specimens represent the late survivors of a Levantine Middle Pleistocene paleodeme that was most likely involved in the evolution of the Middle Pleistocene *Homo* in Europe and East Asia.

Recent dental (*1*), mandibular (*2*), genetic (*3*, *4*), and demographic (*5*) studies have predicted the existence of an as yet unidentified African or West Asian Middle Pleistocene (MP) population that contributed to the evolution of the Neanderthal clade. This contrasts with the traditional view that considered the European continent as the sole place of origin of the Neanderthals and their direct ancestors.

Here we report on the discovery of several fossils from the recently excavated MP open-air site of Nesher Ramla (NR), central Israel (Fig. 1), in association with stone artifacts, and faunal remains (*6*).

A nearly complete right parietal bone and four fragments from the left parietal bone represent the NR-1 fossil (Fig. 2A and fig. S1). The NR-2 fossil is an almost complete mandible, missing only the left ramus, the right condylar process, and the mandibular angle of the right ramus (Fig. 3). The lower left second molar (NR-2 M_2) and most of the dental roots are still in place (fig. S2). Both NR-1 and NR-2 were found in situ within the lowest archaeological layer (Fig. 1D, Unit VI), together with animal bones and flint tools, and most likely represent the same individual (supplementary text A).

Unit VI is assigned an age of 140 to 120 thousand years (ka) ago, based on the electron spin resonance–uranium series (ESR-US) dates of animal teeth recovered in this unit (with a weighted mean of 125.8 ± 5.9 ka). This age was corroborated by a series of thermoluminescence (TL) dates of burnt flints from the archaeological layer immediately above the fossil (Unit V). This layer yielded a weighted mean of 127.6 ± 4.0 ka (confirmed by isochron analysis), which is in agreement with the ESR-US dates obtained for this unit, ranging between ~128 and ~120 ka (a weighted mean of 122.3 ± 3.3 ka). This chronological information is consistent with the previously published optically stimulated luminescence (OSL) dates for the entire archaeological sequence [ranging ~170 and ~78 ka; (*6*)].

The preserved anatomical elements were thoroughly described and analyzed in comparison to a large number of fossils of different periods (table S1), using a combination of traditional approaches based on linear and angular measurements, as well as three-dimensional (3D) landmark-based geometric morphometric (GM) methods (supplementary text C to E).

The overall morphology of the NR-1 parietal bones (supplementary text C and tables S2 and S3) is indicative of an archaic, low cranial vault, which is typical of MP *Homo* specimens and is substantially different from early and recent *H. sapiens*, which instead manifest a curved parietal bone with a pronounced eminence (*7*, *8*).

Further support for the rather archaic morphology of the NR *Homo* comes from the angle formed by the coronal and sagittal sutures (c/s angle), 91.1° in the NR-1 specimen. This angle increased during the evolution of Pleistocene *Homo* (fig. S3): *H. erectus* and African MP *Homo* exhibit a mean angle of 92.1° ± 2.1°; the angle opens to 94.9° ± 3.4° in European MP *Homo*/Neanderthals and reaches 99.4° ± 4.2° in early and recent *H. sapiens*. The c/s angle is significantly different between these three groups (*H* = 22.5, *p* < 0.001). The c/s angle for NR-1 is similar to that of archaic *Homo*, particularly African MP *Homo* (91.1° ± 1.1°), and falls outside the range of variation of *H. sapiens*.

The NR-1 parietal bone is considerably thick, mainly in the parietal eminence area (figs. S4 and S5). Regarding this aspect, the NR-1 parietal is similar to that of European MP *Homo* specimens (e.g., Petralona, Atapuerca SH) (fig. S4). It is generally thicker than the parietal of Neanderthals (e.g., Amud 1, Guattari, and La Chapelle-aux-Saints) and most early *H. sapiens* (except for Laetoli H18 and Omo 2), and it is much thicker than that of recent *H. sapiens*.

The 3D GM analysis, used to assess NR-1 shape variation with respect to a comparative sample of Pleistocene and recent *Homo* (supplementary text, Fig. 2C, fig. S1, and table S1), confirms the archaic morphology of NR-1. The first three principal components (PCs) explain 74.5% of the total shape variance. The first PC (34.9%) differentiates early and recent *H. sapiens* from all other groups, including Asian *H. erectus*, European and African MP *Homo,* and Neanderthals, owing to their marked curvature along both the sagittal and the coronal planes (Fig. 2C). The second PC (21.3%) is not taxonomically informative (fig. S1). The third PC (18.3%) separates Asian *H. erectus* and African MP *Homo* from Neanderthals and European MP *Homo* (Fig. 2C), based on the relative development of the parietal eminence and its relative antero-posterior position. The European MP group is characterized by an antero-posteriorly and supero-inferiorly flatter parietal bone (Fig. 2C). NR-1 is distinct from *H. sapiens*; it is at an intermediate position between the Neanderthal and MP *Homo* clusters (Fig. 2C). An unrooted phylogenetic analysis, based on the mean shape of each *Homo* group, placed NR-1 close to the origin of the branch

[1]Department of Anatomy and Anthropology, Sackler Faculty of Medicine, Tel Aviv University, Tel Aviv, Israel. [2]The Shmunis Family Anthropology Institute, the Dan David Center for Human Evolution and Biohistory Research, Sackler Faculty of Medicine, Tel Aviv University, Tel Aviv, Israel. [3]Department of Oral Biology, the Goldschleger School of Dental Medicine, Sackler Faculty of Medicine, Tel Aviv University, Tel Aviv, Israel. [4]UMR7194, HNHP, Département Homme et Environnement, Muséum national d'Histoire naturelle, CNRS, UPVD, Paris, France. [5]CENIEH (National Research Center on Human Evolution), Burgos, Spain. [6]Institute of Evolutionary Medicine, University of Zurich, Zurich, Switzerland. [7]Department of Evolutionary Anthropology, University of Vienna, Vienna, Austria. [8]Department of Anthropology, Binghamton University (SUNY), Binghamton, NY, USA. [9]Centro UCM-ISCIII de Evolución y Comportamiento Humanos, Madrid, Spain. [10]Division of Anthropology, American Museum of Natural History, New York, NY, USA. [11]Departamento de Geodinámica, Estratigrafía y Paleontología, Facultad de Ciencias Geológicas, Universidad Complutense de Madrid, Ciudad Universitaria s/n, 28040, Madrid, Spain. [12]Department of Anthropology, University College London, London, UK. [13]Department of Human Molecular Genetics and Biochemistry, Sackler Faculty of Medicine, Tel Aviv University, Tel Aviv, Israel. [14]PalaeoHub, Department of Archaeology, University of York, York, UK. [15]Thuringian State Office for the Preservation of Historical Monuments and Archaeology Weimar, Germany. [16]Department of Environmental Biology, Sapienza University of Rome, Roma, Italy. [17]Core Facility for Micro-Computed Tomography, University of Vienna, Vienna, Austria. [18]Institute of Archaeology, The Hebrew University of Jerusalem, Jerusalem, Israel. [19]Zinman Institute of Archaeology, University of Haifa, Haifa, Mount Carmel, Israel.

*Corresponding author. Email: anatom2@tauex.tau.ac.il (I.H.); mayhila@tauex.tau.ac.il (H.M.); sarigrac@tauex.tau.ac.il (R.S.) †These authors contributed equally to this work. ‡Present address: Natural History Museum, University of Florence, Florence, Italy.

leading to African MP *Homo*, close to the split from the *H. erectus* branch and to European MP *Homo* and Neanderthals (including Atapuerca SH), and far from early and recent *H. sapiens* (Fig. 2B).

With regard to the configuration of the endoparietal surface (fig. S5), NR-1 is polygonal, i.e., the surface is clearly oriented according to three distinct planes (fig. S5). Instead, Neanderthals and *H. sapiens* manifest an arched endoparietal surface. The flatness of the superior parietal lobule, seen in the NR-1 virtual endocast (fig. S6), is one of the most characteristic features of MP *Homo* (*9*, *10*). Other important characteristics of the NR-1 endocast and that are also typical of MP *Homo* are the very low position of the maximum endocranial width at the superior part of the first temporal convolution (fig. S6), the very short parietal lobe (fig. S7), and the differing lengths of the maximal endocranial width and intraparietal width as well as their posterior position on the parietal bone (table S3). These features can sometimes also be seen in Neanderthals (table S3) (*9*, *10*). Conversely, recent *H. sapiens* specimens exhibit subequal maximal endocranial and intraparietal widths, which are located much higher and more anteriorly than in NR-1 (*9*).

The vascular pattern of the middle meningeal vessels in NR-1 is simple. Only a few, short ramifications are visible and anastomoses are absent, as is the case in other MP *Homo* and Neanderthals (figs. S9 and S10) (*11*). The posterior branch of the middle meningeal vessel in NR-1 is as developed as the anterior one, a pattern persistent among MP *Homo*. Both Neanderthals (e.g., La Quina H5 and La Chapelle-aux-Saints) and recent *H. sapiens* show a dominance of the anterior branch; the latter also possesses complex vascular endocranial imprints (fig. S10).

The NR-2 specimen is a robust mandible (Fig. 3); the corpus is medio-laterally wide, and the cortical bone is thick (Fig. 3, fig. S11). Its most pronounced feature is the short ramus relative to the body height, with a sturdy, low, and wide coronoid process (Fig. 3). This specimen displays several archaic features (e.g., no trigonum mentale or incurvatio mandibulae, a wide incisura submentalis, a developed planum alveolare, a strongly developed planum triangulare, and a mandibular corpus that presents fairly parallel alveolar and basal margins) commonly seen in MP *Homo* (*12*, *13*) (supplementary text D and table S4A).

We combined taxonomically relevant mandibular features into a hierarchical clustering analysis (fig. S12). Modern and Pleistocene humans form the two main clusters: NR-2 is placed on a side branch of the latter, together with MP *Homo* from Atapuerca SH, Tighenif 3, Arago XIII, and one Neanderthal (fig. S12). The discrete traits underscore the mosaic nature of the NR mandible, showing archaic morphology together with some Neanderthal traits.
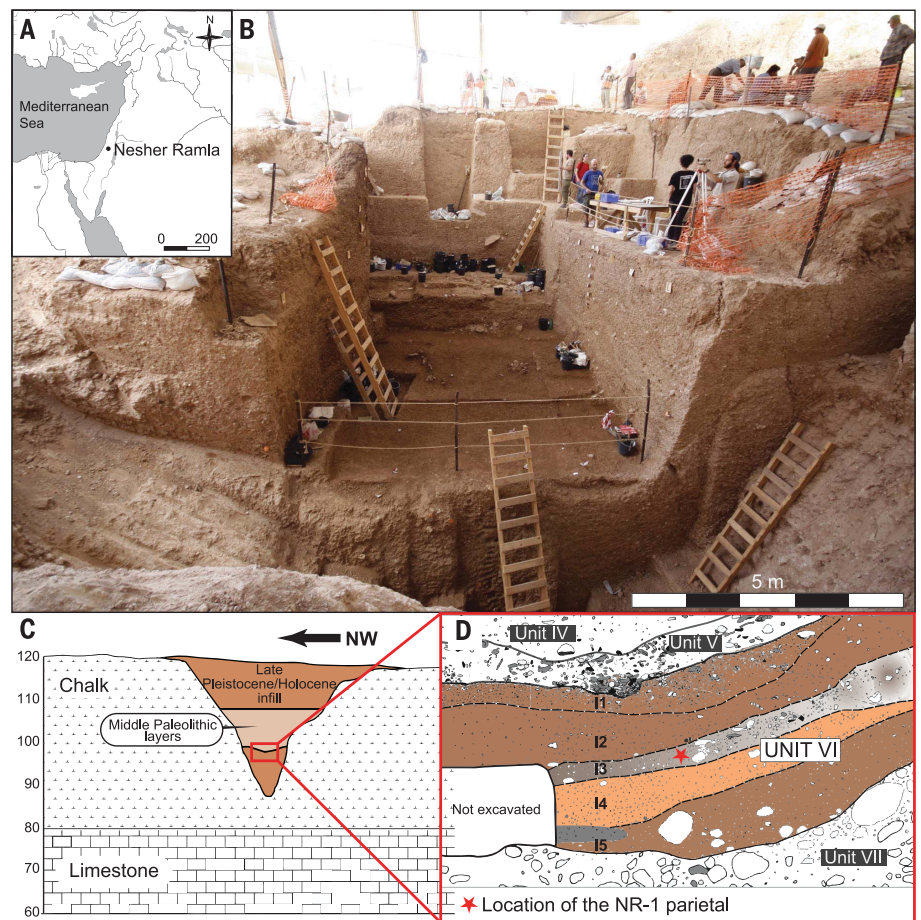

Fig. 1. The Nesher Ramla site and its stratigraphy. (A) Map of the eastern Mediterranean region showing the location of the site. (**B**) View of the excavation from the east. (**C**) Section through the general archaeological sequence placed within the local geology (the vertical scale on the left shows meters above sea level). (**D**) Magnification of Units IV to VII. A red star denotes the location of the NR-1 (parietal bone) 8 m below the surface in Unit VI. NR-2 (mandible) was found in the same unit, 2 m to the north.

The metric dimensions of the NR-2 mandibular body are presented in fig. S13. The symphyseal area is considerably thick (16.6 mm), close to the values of European MP *Homo* mandibles (16.9 ± 2.1 mm), and moderately tall (33.7 mm), close to the Neanderthal mean (34.0 ± 4.6 mm). The body (measured between the first and the second molar) is thick (17.7 mm), within the range of European MP *Homo* (18.1 ± 3.1 mm), yet taller (32.7 mm) than that of European MP *Homo* (30.2 ± 1.6 mm) and Neanderthals (29.9 ± 3.3 mm), close to the values of early *H. sapiens* (33.0 ± 4.0 mm).

The results of the 3D GM analysis (fig. S14 and tables S5A and S5B) for the NR-2 mandible are illustrated in Fig. 3C. The first two principal components explain 47.5% of the total variance. Variation along PC1 (37.9%) is driven by changes in the length of the mandibular body, the shape of the ramus (shorter and broader among archaic *Homo*), and the expression of the mental area. Variation along PC2 (9.6%) reflects changes in the body height

(mainly in the mental region), and the transition from a body's parallel alveolar and basal margins to ones that converge posteriorly. In the PC1-PC2 plot, early and recent *H. sapiens* separate from the other *Homo* specimens, whereas European MP *Homo* and Atapuerca SH are distinguished from Neanderthals (including the Levantine Amud 1) and Asian *H. erectus*. NR-2 falls between Neanderthals and the European MP *Homo* specimens (including Atapuerca SH), far outside the range of the variation of *H. sapiens*. The phylogenetic analysis, based on the mandibular mean shape of each hominin group, placed NR-2 on a separate branch (together with Tabun C1), close to the split between MP European fossils and Neanderthals, and far from *H. erectus*, African MP *Homo*, and *H. sapiens* (Fig. 3B). This result, based on metrics alone, largely echoes the results of the cluster analysis based on discrete traits and confirms that NR-2 belongs to an archaic group with Neanderthal affinities.

The lower second molar (NR-2 M_2) is complete and shows some occlusal wear causing a slight exposure of the dentine horns (Fig. 4A and supplementary text E). The occlusal surface of the NR-2 M_2 reveals four well-developed cusps and a hypoconulid. The presence of five main cusps is typical for most (70%) of the Atapuerca SH Homo (14) and Neanderthals (15). The NR-2 M_2 has a clear continuous mid-trigonid crest and a discontinuous distal trigonid crest on the dentine surface, corresponding to grade 3 of Bailey et al. (16) (fig. S15). A mid-trigonid crest is present in more than 90% of Neanderthals and MP Homo from Atapuerca SH (14, 15). A grade 3 expression of the mid-trigonid crest, as in the NR-2 M_2, is present in nearly 60% of the Neanderthal specimens, but it is absent in H. sapiens (16). The Qesem Cave M_2 specimen (QC-J15) (17) shows a similar pattern of a continuous mid-trigonid crest and a discontinuous distal trigonid crest (fig. S15). The Ehringsdorf G specimen presents only a mid-trigonid crest (but no distal crest) (fig. S15), whereas the Mauer specimen does not manifest a mid-trigonid crest at all.

The NR-2 M_2 has a single, pyramidal root bifurcating at the apical fourth of the root (Fig. 4, C and D). The large pulp cavity extends to the middle of the root and branches out into short root canals that extend into the apices, a configuration of the roots known as taurodontism (Fig. 4). This pyramidal root, with a taurodontic pulp cavity, is frequent in Neanderthals (18). In modern humans, the second lower molars possess separate mesial and distal roots with some variation in the canals. The root of the NR-2 M_2 (Fig. 4 and fig. S15) is relatively long (16.4 mm), falling toward the higher end of the range of the variation of both Upper Paleolithic H. sapiens (11.3 to 16.8 mm) and Neanderthals (14.3 to 16.5 mm).

The 3D GM analysis for the dentinal crown shape (landmark configuration combining the information from the enamel-dentin junction or EDJ, and that from the cemento-enamel junction or CEJ: fig. S16 for the measurement template, table S6 for the landmark definitions, and fig. S17 for the PC1-PC2 plot and the PC1-PC3 plot) showed that the NR-2 M_2 falls at the upper distant margin of the Neanderthal range, close to the Krapina specimens and Ehringsdorf G.

Shape variation along PC1 (30.6% of the total variance) is driven by the relative height of the crown and by the bucco-lingual expansion of the EDJ relative to the dentine outline. Like the M_2 of Neanderthals and H. sapiens, NR-2 M_2 exhibits a relatively high crown and a bucco-lingually expanded EDJ. Along PC2 (14.7%), the NR-2 M_2 plots toward the most extreme range of the distribution, opposite to the H. sapiens, Atapuerca SH, and African MP specimens. The associated shape is characterized by the expansion of the distal aspect of the dentine crown, a feature that NR-2 M_2 shares with some Neanderthal specimens (Krapina and El Sidrón) and the European MP Homo Ehringsdorf G (supplementary text E). Differently from the parietal and mandible, the unrooted phylogenetic trees' construction, based on the combined CEJ-EDJ data (Fig. 4B), resulted in a clear affiliation with Neanderthals, whereas Qesem QC-J15 associated with Atapuerca SH. Concerning crown size, NR2 M_2 is outside the modern human range (fig. S18).

The cumulative evidence from the three analyzed anatomical elements (parietal bone, mandible, and M_2) reveal a unique combination of archaic and Neanderthal features, supporting the existence of a local, Levantine population at the final MP. The results of the
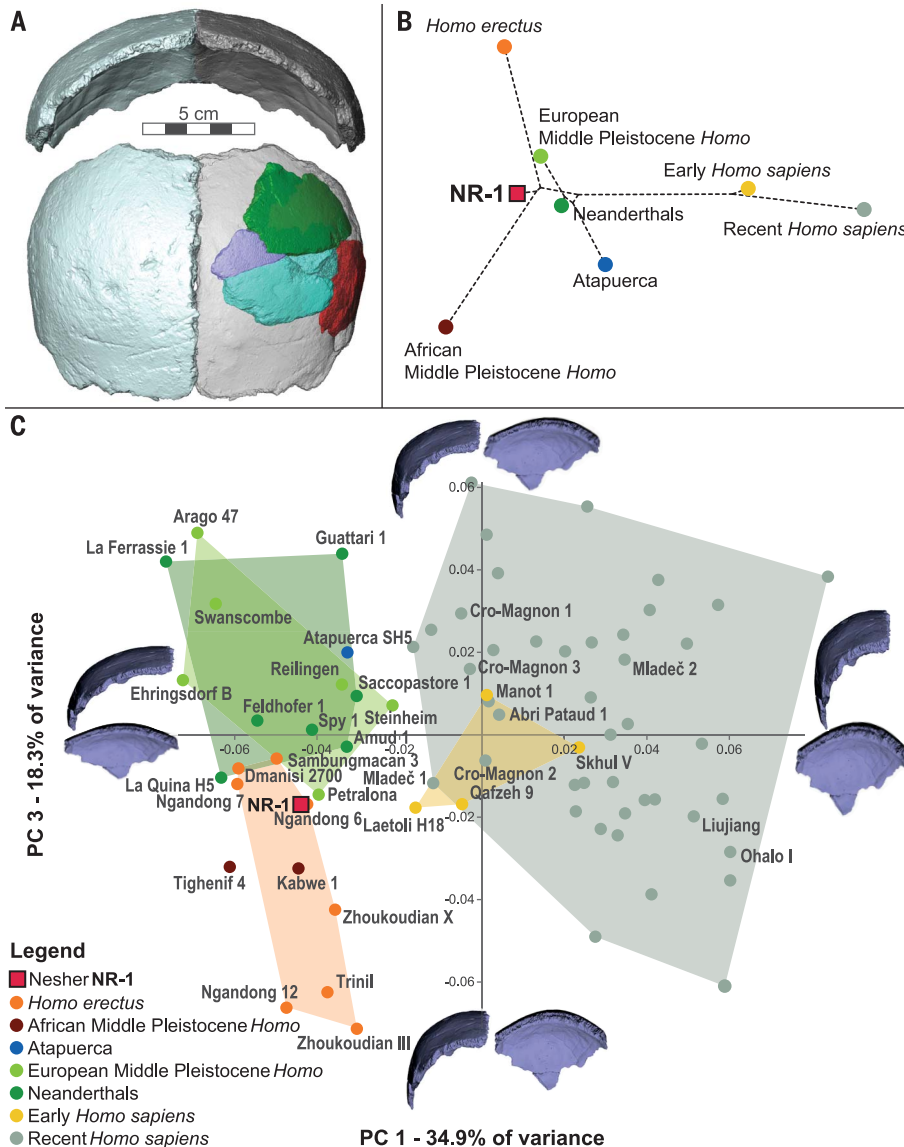

Fig. 2. The NR-1 parietal bones and their analyses. (A) Virtual reconstruction of the middle portion of the calvarium including both parietals. The almost complete right parietal was mirrored-imaged and the left parietal fragments (represented in various colors) were superimposed, showing a very good overlap with the contralateral part. **(B)** An unrooted phylogenetic tree constructed on the mean shape of each group using the neighbor-joining method. NR-1 is positioned on the line leading to African MP Homo, close to the splitting point from H. erectus and not far from the European MP Homo and Neanderthals. **(C)** PCA plot in shape space for the parietal bone. PC1 separates early and recent H. sapiens from the rest of the Homo sample. European MP Homo and Neanderthals (including the Levantine Amud 1) overlap and are distinguished from Asian H. erectus and African MP Homo along PC3; NR-1 is intermediate between these clusters and is close to Petralona and some late Asian H. erectus. Extreme shapes along the PCs are shown from the anterior and medial views.

quadratic discriminant analyses (QDAs) (table S7) reinforce this observation, showing that an affiliation of the NR fossils with early and recent *H. sapiens* is highly unlikely, but that it is impossible to establish whether NR fossils are more likely to be classified as MP *Homo*, Neanderthal, or *H. erectus* (the latter for the parietal only). Consequently, the discriminant function plot (fig. S1) shows that the NR-1 parietal falls between the *H. erectus*/African MP *Homo* group and the European MP *Homo*/Neanderthals, with a similar likelihood of belonging to either cluster (*H. erectus* = 0.41, MP *Homo* = 0.34, Neanderthal = 0.25, based on the first three PCs).

The earliest that Neanderthal features in Levantine fossils have been discernible in the MP was around 400 ka ago at Qesem Cave (*19*), the earliest modern humans were present in the Levant around 180 ka ago (*20*), and unequivocal Neanderthals did not appear in the Middle East before ~70 ka ago. NR bridges a gap in this record, by displaying a highly heterogeneous, yet archaic morphology. The parietal documents a rather archaic shape of the braincase; the mandible is similar to that of MP *Homo*; the molar is quite Neanderthal-like, similar to Ehringsdorf G.

Arsuaga *et al.* (*21*) advocated an earlier evolutionary development of the masticatory apparatus, compared with the braincase in Neanderthals. Similarly, the Jebel Irhoud fossils from North Africa possess a more primitive neurocranium but a more *H. sapiens*–like face and dentition (*22*). Archaic populations carrying Neanderthal-like features were also present across much of the Eurasian continent during the MP, revealed by the Chinese findings of Maba, Xujiayao, and Xuchang (*23–27*). The existence of MP Asian populations deviating markedly from the *H. erectus* paradigm has been repeatedly proposed, for instance, for the Tongzi teeth (*28*) or the Sambungmacan 3 cranium (*29*); the latter (together with Ngandong 6 and 7) shows strong morphological affinities with the NR-1 parietals.

The NR fossils could represent late-surviving examples (140 to 120 ka) of a distinctive Southwest Asian MP *Homo* group, predating Levantine Neanderthals from Amud, Kebara, and Ein Qashish (70 to 50 ka). On the basis of their mosaic morphology showing a different degree of Neanderthal features, other MP Levantine fossils, whose taxonomic affinities have long been debated, from the sites of Qesem Cave (*19*), Zuttiyeh Cave (*30*), and probably Tabun Cave (*31*), might also be attributed to this group (supplementary text F). Adopting the cautious approach advocated by Mayr (*32*), we suggest addressing this Levantine MP paleodeme as the "Nesher Ramla *Homo*." Its presence from ~420 to 120 ka ago in a geographically restricted area may have allowed for repeated interbreeding with modern
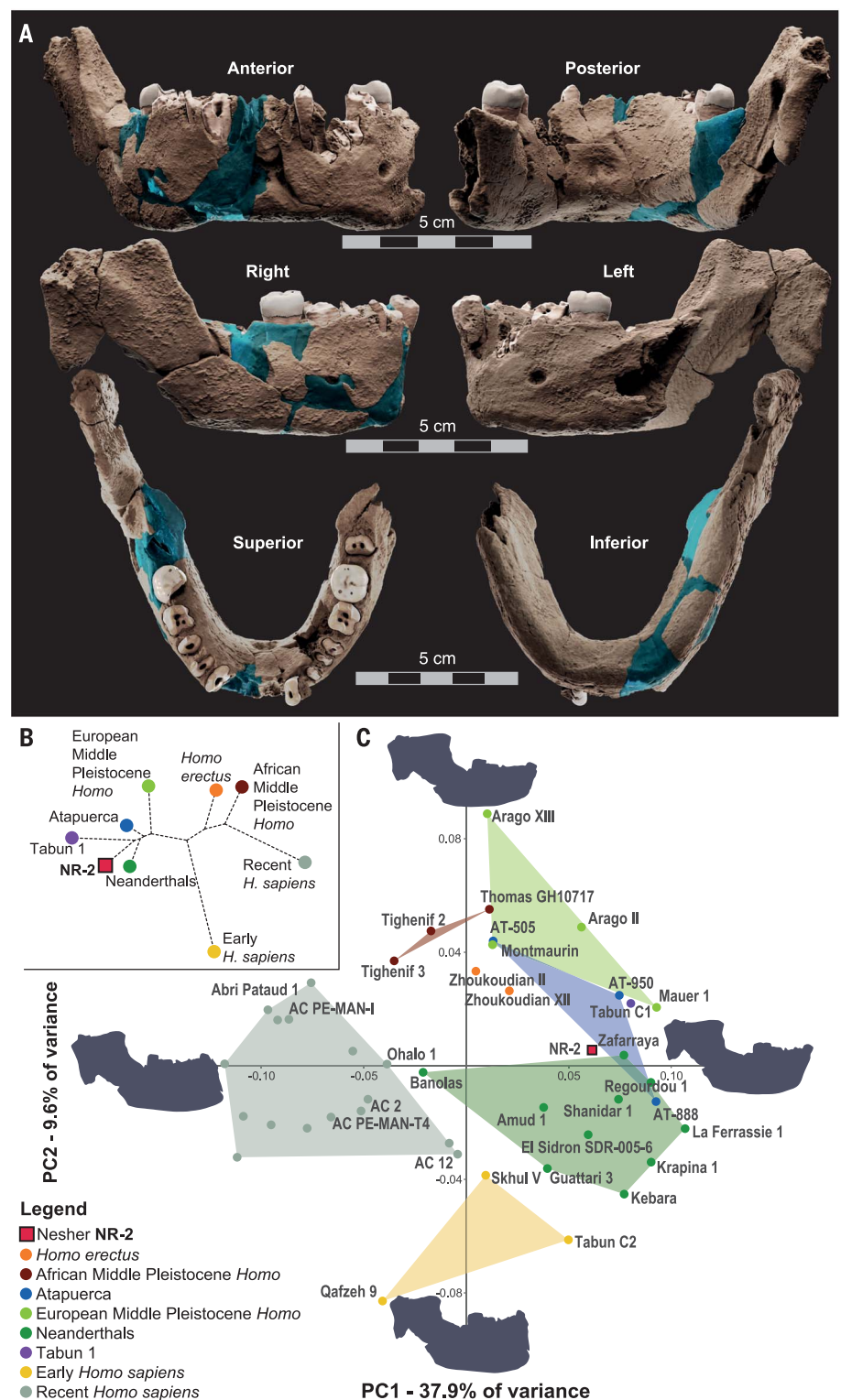
Fig. 3. The NR-2 mandible and its analysis. (**A**) Different views of the reconstructed mandible. (**B**) Unrooted phylogenetic tree constructed using the mean shape of each *Homo* group using the neighbor-joining method. NR-2 and Tabun C1 have a common ancestor that is close to the split between Neanderthals and European MP *Homo* and far from early and recent *H. sapiens*, as well as from *H. erectus* and African MP *Homo*. (**C**) PCA plot for the mandible in shape space. The combination of PC1 and PC2 separates early and recent *H. sapiens* from the other *Homo* specimens and distinguishes European MP *Homo* and Atapuerca from Neanderthals (including the Levantine Amud 1) and Asian *H. erectus*. NR-2 plots between Neanderthals and European MP *Homo*. Extreme shapes along PC1 and PC2 are shown from a lateral view.
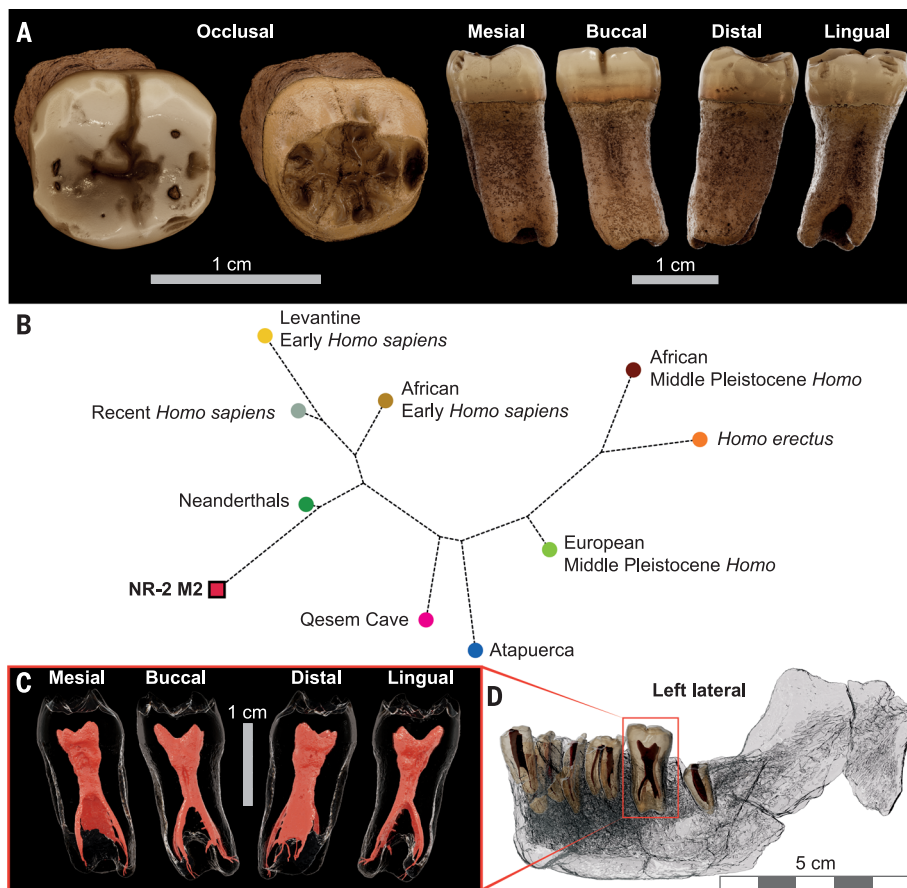
Fig. 4. The lower left second molar (NR2 M₂) and its analysis. (**A**) From the left, the NR2 M₂ in an occlusal view, with and without an enamel cap, and in mesial, buccal, distal, and lingual views. The mesial and distal interproximal wear facets are visible in the buccal and lingual views. (**B**) An unrooted phylogenetic tree construction, based on the mean shape of each hominin group using the neighbor-joining method. NR2 M₂ is close to Neanderthals and far from *H. sapiens*. (**C**) Root canals (pulp cavities) in the mesial, buccal, distal, and lingual views. The pyramidal roots and the taurodontic pulp cavity extend into the apex before branching out into short root canals. (**D**) The dental roots (in brown) and their canals (in red) are presented in "glass" images of the mandible from a lateral view, revealing the presence of taurodontism.

human populations such as the people from Misliya Cave (*20*), a notion also supported by their shared technological tradition [(*6*); supplementary text F]. This scenario is compatible with evidence of an early (200 to 400 ka ago) gene flow between modern humans and Neanderthals (*3, 4*) and helps explain the variable expression of the dental and skeletal features of later Levantine fossils from the Skhul and Qafzeh populations, a phenomenon noted by anthropologists since the 1930s (*31, 33*). Moreover, a recent study of the Atapuerca SH and Arago dental remains (*1*) suggested the existence of more than one *Homo* lineage in MP Europe [see also (*34*)] and hypothesized the contribution of Levantine *Homo* groups carrying Neanderthal-like traits to European *Homo* lineages. The NR *Homo*, carrying Neanderthal-like traits, could thus represent the "source" population postulated in the demographic "sources and sinks" model (*5*), according to which Western Europe was repopulated through a series of successive migrations.

REFERENCES AND NOTES

1. J. M. Bermúdez de Castro *et al.*, *Quat. Sci. Rev.* **217**, 45–61 (2019).
2. M. Roksandic, P. Radović, J. Lindal, *Quat. Int.* **466**, 66–81 (2018).
3. C. Posth *et al.*, *Nat. Commun.* **8**, 16046 (2017).
4. M. Meyer *et al.*, *Nature* **531**, 504–507 (2016).
5. R. W. Dennell, M. Martinón-Torres, J. M. Bermúdez de Castro, *Quat. Sci. Rev.* **30**, 1511–1524 (2011).
6. Y. Zaidner *et al.*, *Science* **372**, 1429–1433 (2021).
7. E. Bruner *et al.*, *Coll. Antropol.* **28**, 99–112 (2004).
8. P. Gunz, S. Neubauer, B. Maureille, J.-J. Hublin, *Curr. Biol.* **20**, R921–R922 (2010).
9. D. Grimaud-Hervé, L'évolution de l'encéphale chez *Homo erectus* et *Homo sapiens*: Exemples de l'Asie et de l'Europe. *Cah. paléoanthropologie* (CNRS éditions, 1997).
10. E. M. Poza-Rey, A. Gómez-Robles, J. L. Arsuaga, *J. Hum. Evol.* **129**, 67–90 (2019).
11. E. Bruner, S. Mantini, A. Perna, C. Maffei, G. Manzi, *Eur. J. Morphol.* **42**, 217–224 (2005).
12. A. Vialet, M. Modesto-Mata, M. Martinón-Torres, M. Martínez de Pinillos, J.-M. Bermúdez de Castro, *PLOS ONE* **13**, e0189714 (2018).
13. A. Mounier, F. Marchal, S. Condemi, *J. Hum. Evol.* **56**, 219–246 (2009).
14. M. Martinón-Torres, J. M. Bermúdez de Castro, A. Gómez-Robles, L. Prado-Simón, J. L. Arsuaga, *J. Hum. Evol.* **62**, 7–58 (2012).
15. S. Bailey, *Period. Biol.* **108**, 253–267 (2006).
16. S. E. Bailey, M. M. Skinner, J. J. Hublin, *Am. J. Phys. Anthropol.* **145**, 505–518 (2011).
17. I. Hershkovitz *et al.*, *Quat. Int.* **398**, 148–158 (2016).
18. K. Kupczik, J.-J. Hublin, *J. Hum. Evol.* **59**, 525–541 (2010).
19. I. Hershkovitz *et al.*, *Am. J. Phys. Anthropol.* **144**, 575–592 (2011).
20. I. Hershkovitz *et al.*, *Science* **359**, 456–459 (2018).
21. J. L. Arsuaga *et al.*, *Science* **344**, 1358–1363 (2014).
22. J.-J. Hublin *et al.*, *Nature* **546**, 289–292 (2017).
23. X. J. Wu, E. Bruner, *Am. J. Phys. Anthropol.* **160**, 633–643 (2016).
24. X.-J. Wu, I. Crevecoeur, W. Liu, S. Xing, E. Trinkaus, *Proc. Natl. Acad. Sci. U.S.A.* **111**, 10509–10513 (2014).
25. Z.-Y. Li *et al.*, *Science* **355**, 969–972 (2017).
26. S. Xing, M. Martinón-Torres, J. M. Bermúdez de Castro, X. Wu, W. Liu, *Am. J. Phys. Anthropol.* **156**, 224–240 (2015).
27. W. Liu *et al.*, *J. Hum. Evol.* **64**, 337–355 (2013).
28. S. Xing, M. Martinón-Torres, J. M. Bermúdez de Castro, *J. Hum. Evol.* **130**, 96–108 (2019).
29. S. Márquez, K. Mowbray, G. J. Sawyer, T. Jacob, A. Silvers, *Anat. Rec.* **262**, 344–368 (2001).
30. S. E. Freidline, P. Gunz, I. Janković, K. Harvati, J. J. Hublin, *J. Hum. Evol.* **62**, 225–241 (2012).
31. A.-M. Tillier, *J. Isr. Prehist. Soc.* **35**, 439–450 (2005).
32. E. Mayr, in *Cold Spring Harbor Symposia on Quantitative Biology* (Cold Spring Harbor Laboratory Press, 1950), vol. 15, pp. 109–118.
33. B. Arensburg, A. Belfer-Cohen, in *Neandertals and Modern Humans in Western Asia*, T. Akazawa, K. Aoki, O. Bar-Yosef, Eds. (Plenum, 1998), pp. 311–322.
34. G. Manzi, *Quat. Int.* **411**, 254–261 (2016).

Science

A Middle Pleistocene *Homo* from Nesher Ramla, Israel

Israel Hershkovitz, Hila May, Rachel Sarig, Ariel Pokhojaev, Dominique Grimaud-Hervé, Emiliano Bruner, Cinzia Fornai, Rolf Quam, Juan Luis Arsuaga, Viktoria A. Krenn, Maria Martinón-Torres, José María Bermúdez de Castro, Laura Martín-Francés, Viviane Slon, Lou Albessard-Ball, Amélie Vialet, Tim Schüler, Giorgio Manzi, Antonio Profico, Fabio Di Vincenzo, Gerhard W. Weber and Yossi Zaidner

Science **372** (6549), 1424-1428.
DOI: 10.1126/science.abh3169

Middle Pleistocene *Homo* in the Levant

Our understanding of the origin, distribution, and evolution of early humans and their close relatives has been greatly refined by recent new information. Adding to this trend, Hershkovitz *et al.* have uncovered evidence of a previously unknown archaic *Homo* population, the ''Nesher Ramla *Homo*'' (see the Perspective by Mirazon Lahr). The authors present comprehensive qualitative and quantitative analyses of fossilized remains from a site in Israel dated to 140,000 to 120,000 years ago indicating the presence of a previously unrecognized group of hominins representing the last surviving populations of Middle Pleistocene *Homo* in Europe, southwest Asia, and Africa. In a companion paper, Zaidner *et al.* present the radiometric ages, stone tool assemblages, faunal assemblages, and other behavioral and environmental data associated with these fossils. This evidence shows that these hominins had fully mastered technology that until only recently was linked to either *Homo sapiens* or Neanderthals. Nesher Ramla *Homo* was an efficient hunter of large and small game, used wood for fuel, cooked or roasted meat, and maintained fires. These findings provide archaeological support for cultural interactions between different human lineages during the Middle Paleolithic, suggesting that admixture between Middle Pleistocene *Homo* and *H. sapiens* had already occurred by this time.

Science, abh3169 and abh3020, this issue p. 1424 and p. 1429; see also abj3077, p. 1395

Downloaded from http://science.sciencemag.org/ on July 27, 2021

ARTICLE TOOLS	http://science.sciencemag.org/content/372/6549/1424
SUPPLEMENTARY MATERIALS	http://science.sciencemag.org/content/suppl/2021/06/23/372.6549.1424.DC1
RELATED CONTENT	http://science.sciencemag.org/content/sci/372/6549/1395.full http://science.sciencemag.org/content/sci/372/6549/1429.full
REFERENCES	This article cites 105 articles, 10 of which you can access for free http://science.sciencemag.org/content/372/6549/1424#BIBL

Use of this article is subject to the Terms of Service

Science (print ISSN 0036-8075; online ISSN 1095-9203) is published by the American Association for the Advancement of Science, 1200 New York Avenue NW, Washington, DC 20005. The title *Science* is a registered trademark of AAAS.

Copyright © 2021 The Authors, some rights reserved; exclusive licensee American Association for the Advancement of Science. No claim to original U.S. Government Works

Use of this article is subject to the Terms of Service